Submitted: 10 July, 2023 Accepted: 23 August, 2023 Published: 15 April, 2025 DOI:10.22514/ejgo.2025.048

ORIGINAL RESEARCH

European Journal of Gynaecological Oncology

Cuproptosis-related gene biomarkers to predict overall survival outcomes in cervical cancer

Hualin Song[1,2,3,†], Yanxiang Cao[4,†], Yishuai Li[5], Miaomiao Liu[6], Huijuan Wu[1,2,3], Ying Chen[1,2,3], Wenxin Liu[1,2,3], Ke Wang[1,2,3], Xin Fu[1,2,3,*]

[1]Department of Gynecological Oncology, Tianjin Medical University Cancer Institute and Hospital, National Clinical Research Center for Cancer, 300060 Tianjin, China
[2]Key Laboratory of Cancer Prevention and Therapy, 300060 Tianjin, China
[3]Tianjin's Clinical Research Center for Cancer, 300060 Tianjin, China
[4]Department of General Surgery, the Second Medical Center, Chinese PLA General Hospital, 100853 Beijing, China
[5]Department of Thoracic Surgery, Hebei Chest Hospital, 050000 Shijiazhuang, Hebei, China
[6]The Fifth Department of Oncology, Hebei General Hospital, 050000 Shijiazhuang, Hebei, China

***Correspondence**
xinfu@tmu.edu.cn
(Xin Fu)

† These authors contributed equally.

Abstract

Background: Cervical carcinoma (CC) remains a prevailing gynecologic malignancy. Cuproptosis is a recently identified and extensively researched type of cellular death. However, the understanding of cuproptosis-associated genes in CC and their correlation with prognosis is still uncertain. **Methods**: We identified 6 genes related to cuproptosis that were differentially expressed between normal cervical tissue and CC from 18 cuproptosis-related genes. We obtained prognostic information, along with associated clinical information, in normal cervical tissue and CCs from TCGA (The Cancer Genome Atlas). **Results**: Six differentially expressed cuproptosis-associated genes were utilized to develop a prognostic pattern and categorize the overall CC patients in the TCGA cohort into low- or high-cohort groups. Gene Expression Omnibus (GEO) database data were employed to certify the model of prognosis. There was a significantly higher survival rate for CC patients in low-risk than in high-risk group ($p = 0.001$) for the TCGA cohort. Both univariate ($p = 0.0012$) and multivariate Cox regression analyses ($p < 0.001$) illustrated that the risk score was obviously linked to poor survival. The outside validation was carried out by data in GEO database. There also existed an exceedingly obvious distinction in the survival rate between the two groups ($p = 0.0239$). There were also evident differences between poor survival and risk score in univariate ($p = 0.0242$) as well as multivariate Cox regression analysis ($p = 0.0279$). KEGG (Kyoto Encyclopedia of Genes and Genomes) and GO (Gene Ontology) were utilized. The results forecasted that extracellular matrix organization, signaling receptor activator activity, receptor ligand activity, neuroactive ligand-receptor interplay, and cytokine-cytokine receptor interplay were closely associated with CC cuproptosis. **Conclusions**: The risk prediction model based on genes related to cuproptosis could excellently predict CC prognosis. The prognostic model can offer a vital reference for future biomarkers and therapeutic targets for the sake of precise therapy of cervical carcinoma.

Keywords

Cervical cancer; Cuproptosis; Risk model; Prognosis; Overall survival

1. Introduction

Globally, cervical cancer ranks fourth after breast, colorectal and lung cancers, and first among gynecological cancers [1, 2]. The CC predominantly occurs because of the persistent presence of high-risk human papillomavirus (HPV). However, HPV infection alone is not the only reason for CC onset and progression [3]. It has been reported that 15% to 61% CC patients have distant or lymph node metastasis in the diagnosis period. Above 70% CC patients have parametrial infiltration or metastasis in diagnosis period and cannot be surgically treated [4]. The curative approaches including chemotherapy and radiotherapy are employed wherein the prognosis of patients is reduced [4]. HPV vaccine has been administered in various countries, however the medical treatment *via* chemotherapy, radiotherapy and surgery has excelled. CC morbidity and mortality can decline in future, but its recurrence, metastasis and drug resistance are challenging [5, 6].

The novel mechanism of copper-induced cell death has recently gained attention [7]. Tsvetkov *et al.* [7] has investigated that the abundance of intracellular copper induces the formation of lipoylated DLAT (dihydrolipoamide S-acetyltransferase) which plays a role in the mitochondrial tricarboxylic acid (TCA) synthesis cycle. This has emerged as a form of cellular death named as "cuproptosis" [7]. Common mammalian cells death modes include apoptosis, necrosis, ferroptosis, necroptosis and autophagy-related death. Earlier studies reveal that pyroptosis, ferroptosis and necroptosis plays a role in the progression of CCs and other gynecological cancers [8–10]. Ferroptosis as a component of programmed cellular death is named because of the role of iron in this process [11]. Copper as a trace metal in

the cells maintains protein function. Copper also mediates the cell death; however its specific mechanism is not well understood as the cuproptosis has been discovered recently [12]. According to Tsvetkov *et al*. [7], the copper ionophore used for treating carcinoma causes cell death when combined with copper, although elesclomol does not have the same effect. This suggests that copper toxicity causes cell death [7, 13, 14]. The copper-induced cellular death systems and antitumor theragnostic utilization of copper compounds are further explored [15]. There can be a link between cuproptosis and cancer, and can take the lead in cancerous advancements, however this connection is still unclear. Studies are required to explore whether cuproptosis is related to CC and has a role in its appearance and progression, and whether cuproptosis related genes can function as prognostic markers of CCs.

Herein, the clinical data and RNA expression of normal cervix were obtained from The Cancer Genome Atlas (TCGA) and the Genotype Tissue Expression (GTEx) database, along with CC tumor tissue from TCGA. Cuproptosis associated genes were identified and classified from published studies [7]. A systematic study was conducted by constructing a predictive model to identify the expression levels of cuproptosis related genes in CCs and normal cervical tissues, and to investigate the prognostic value of the model. The Kaplan-Meier (KM) curve, area under the curve (AUC) and forest plot indicated that the model had good prognostic performance. Another part of CC patient tumor tissue was obtained through Gene Expression Omnibus (GEO) database to validate the model. KM, AUC, and forest plots reflected that the pattern had prognostic performance among the validation cohort. Finally, the functional enrichment analysis was performed on the differentially expressed genes in high- and low-risk groups of the model to investigate potential gene action mechanisms.

2. Methods

2.1 Dataset acquisition

We sequenced (RNA-seq) 306 cervical cancer patients and three normal cervical tissues with corresponding clinical data from the TCGA database on 15 March 2022. Data for ten human normal cervical tissue samples were obtained from the GTEx database. The external validation of CC patient RNA-seq coupled with relevant clinical information originated from the GEO database (ID: GSE30759).

2.2 Identification of differentially expressed cuproptosis-related genes

Eighteen cellular cuproptosis associated genes from literature were extracted: *Lipoyltransferase 1* (*LIPT1*), *Ferredoxin 1* (*FDX1*), *ATPase Copper Transporting Beta* (*ATP7B*), *Dihydrolipoamide Dehydrogenase* (*DLD*), *Lipoic Acid Synthetase* (*LIAS*), *Glycine Cleavage System Protein H* (*GCSH*), *Dihydrolipoamide Branched Chain Transacylase* (*DBT*), *Dihydrolipoamide S-Acetyltransferase* (*DLAT*), *Dihydrolipoamide S-Succinyltransferase* (*DLST*), *Pyruvate Dehydrogenase E1 Subunit Beta* (*PDHB*), *Pyruvate Dehydrogenase E1 Subunit Alpha 1* (*PDHA1*), *ATPase Copper Transporting Alpha* (*ATP7A*), *Solute Carrier Family 31 Member 1* (*SLC31A1*), *Succinate Dehydrogenase Complex Iron Sulfur Subunit B* (*SDHB*), *Polymerase Delta 1* (*POLD1*), *NADH*: *Ubiquinone Oxidoreductase Subunit B8* (*NDUFB8*), *Translocase Of Outer Mitochondrial Membrane 20* (*TOMM20*) and Dihydropyrimidine Dehydrogenase (*DPYD*) [7]. The data of only three cases of normal cervical tissue from TCGA cohort, and that of ten normal cervical samples from GTEx database were obtained for identifying the differentially expressed genes (DEGs). The "limma" package was used to identify DEGs with p values 0.05. The protein-protein interaction (PPI) network for cuproptosis-associated genes was set up by using STRING (Search Tool for Retrieving Interacting Genes), version 11.5 (https://string-db.org/).

2.3 Development and validation of cuproptosis-related gene prognostic model

The association between cuproptosis-related genes and survival in TCGA was studied by Cox regression analysis. p value was fixed at 0.2 to stop the omission, wherein six genes related to survival were identified for further study. The Least Absolute Shrinkage and Selection Operator (LASSO) was chosen to recognize the candidate genes and boost one prognostic model. Six cuproptosis-associated genes and their coefficients were retained (λ), and the minimum criterion was used to determine the penalty parameter. TCGA expression dataset was utilized to determine the risk score by following the normalization through "scale" function in R (Version 4.2.3, Lucent Technologies, Paris, France). Risk score was calculated by risk score = P7i Xi Yi (X coefficient, Y gene expression grade). TCGA CCs were categorized as high- and low-risk subgroups based on median risk scores. The overall survival (OS) time was compared with Kaplan-Meier analysis for two subgroups. ROC curve analysis at 1, 2 and 5 years was conducted *via* the R packages "survminer", "survival" and "time-receiver operating characteristic (ROC)". CC cohort from GEO database (ID GSE30759) was employed for validation. Moreover, individuals from GSE30759 were divided into high- and low-risk subgroups. The groups were then compared to validate the risk model.

2.4 Independent prognostic analysis of the risk model

The data about grade and age were extracted from TCGA and GEO. The model herein analyzed these variables along with risk score. The multivariate and univariate Cox regression models were used for analysis.

2.5 Functional enrichment analysis of DEGs for low- and high-risk groups

DEGs were divided into two subgroups based on specific criteria (false discovery rate (FDR) <0.05 and log2FC ≥ 1). The KEGG and GO examinations of DEGs were conducted on clusterProfiler software [16].

2.6 Statistical analysis

One-way analysis of variance (ANOVA) was used to compare the gene expression levels between typical cervical tissue and

CC, while Pearson's chi-square test was used to compare categorical variables. To compare the operating systems among the subcategories, we utilized two-sided log-rank and Kaplan-Meier tests. Multivariate and univariate Cox regression patterns were employed to assess the autonomous prognostic significance of the risk models. All statistical analyses were conducted using R software, specifically version 4.0.5. Fig. 1 shows cases the displayed flow chart.

3. Results

3.1 Identification of DEGs for normal and tumor tissues

Fifteen DEGs were identified ($p < 0.05$) despite the contrasting expression levels of 18 cellular cuproptosis linked genes in 306 neoplasm and 13 normal organisms from GTEx and TCGA data. Among them, twelve genes (*TOMM20*, *ATP7A*, *SDHB*, *DLD*, *DPYD*, *LIAS*, *DLST*, *PDHB*, *LIPT1*, *PDHA1*, *GCSH* and *NDUFB8*) were downregulated, and three genes (*SLC31A1*, *POLD1* and *ATP7B*) upregulated in cancer tissues. Fig. 2A depicts a heatmap illustrating mRNA expression levels of these genes. PPI analysis revealed about interactions of cuproptosis-related genes (Fig. 2B). A minimum interaction score of 0.9 was established for analysing PPI (highest confidence), and identified *LIPT1*, *LIAS*, *PHDB*, *GCSH*, *DLAT*, *DLST*, *PDHA1*, *SDHB*, *DBT* and *DLD* as pivotal genes. All genes except *DLAT* and *DBT* exhibited differential expressions between normal and neoplasm tissues. Fig. 2C depicts a network that shows correlation among cuproptosis associated genes.

3.2 DEGs based classification

Consensus clustering analysis was performed on 306 CC patients in TCGA to evaluate the association between expression levels of fifteen cellular cuproptosis-associated DEGs and CC. The intergroup correlation was minimum at k value of 2, while the intragroup correlation was the highest when k increased from 2 to 10, representing the clustering variable. The 306 CC patients were categorized into two groups using 15 DEGs (Fig. 3A). Gene expression profiles and clinical parameters such as age, grade and survival state were presented in the heatmap. There was little difference between the two regarding clinical characteristics among clusters (Fig. 3B). Furthermore, overall survival (OS) times of two clusters were compared and found significant differences ($p = 0.00628$, Fig. 3C).

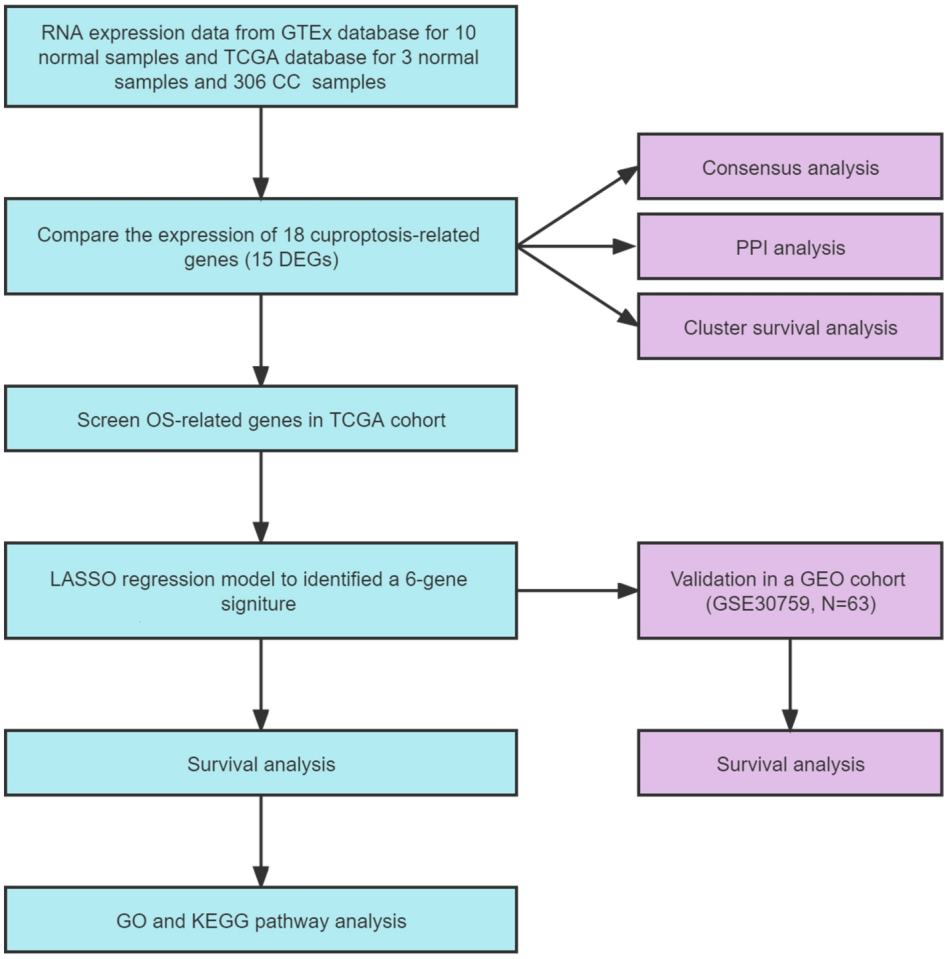

FIGURE 1. The specified workflow picture of information dissection. GTEx: Genotype Tissue Expression; TCGA: The Cancer Genome Atlas; CC: Cervical carcinoma; DEGs: differentially expressed genes; OS: overall survival; LASSO: Least Absolute Shrinkage and Selection Operator; GO: Gene Ontology; KEGG: Kyoto Encyclopedia of Genes and Genomes; PPI: protein-protein interaction; GEO: Gene Expression Omnibus.

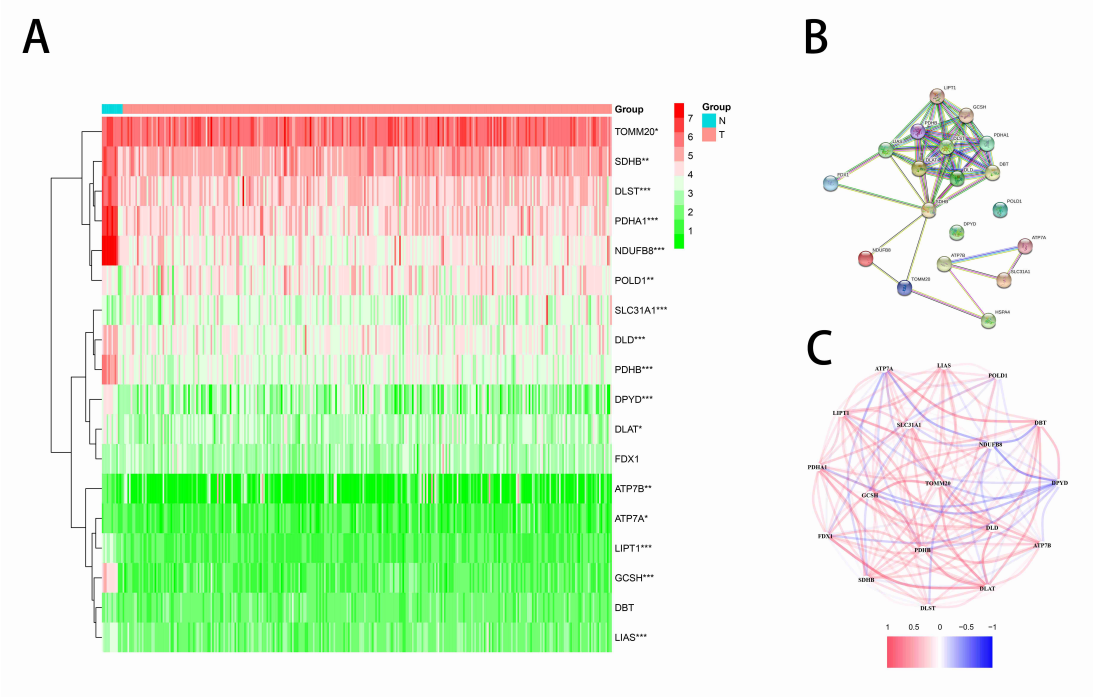

FIGURE 2. Illustrates the expression patterns of eighteen genes associated with cuproptosis and their interactions. (A) heatmap illustrating the variation in gene expression related to cuproptosis between tumor and normal tissues. The *p* values are displayed as ***$p < 0.001$ and **$p < 0.01$. (B) The PPI network showing interactions between genes in cuprotosis (interaction score = 0.9). (C) The network of gene correlations related to cuproptosis (red line: positive relationship; blue line: negative relationship). The intensity of colors indicates the association strength. TOMM20: Translocase Of Outer Mitochondrial Membrane; SDHB: Succinate Dehydrogenase Complex Iron Sulfur Subunit B; DLST: Dihydrolipoamide S-Succinyltransferase; PDHA1: Pyruvate Dehydrogenase E1 Subunit Alpha 1; NDUFB8: NADH:Ubiquinone Oxidoreductase Subunit B8; POLD1: Polymerase Delta 1; SLC31A1: Solute Carrier Family 31 Member 1; DLD: Dihydrolipoamide Dehydrogenase; PDHB: Pyruvate Dehydrogenase E1 Subunit Beta; DPYD: Dihydropyrimidine Dehydrogenase; DLAT: Dihydrolipoamide S-Acetyltransferase; FDX1: Ferredoxin 1; ATP7B: ATPase Copper Transporting Beta; ATP7A: ATPase Copper Transporting Alpha; LIPT1: Lipoyltransferase 1; GCSH: Glycine Cleavage System Protein H; DBT: Dihydrolipoamide Branched Chain Transacylase; LIAS: Lipoic Acid Synthetase.

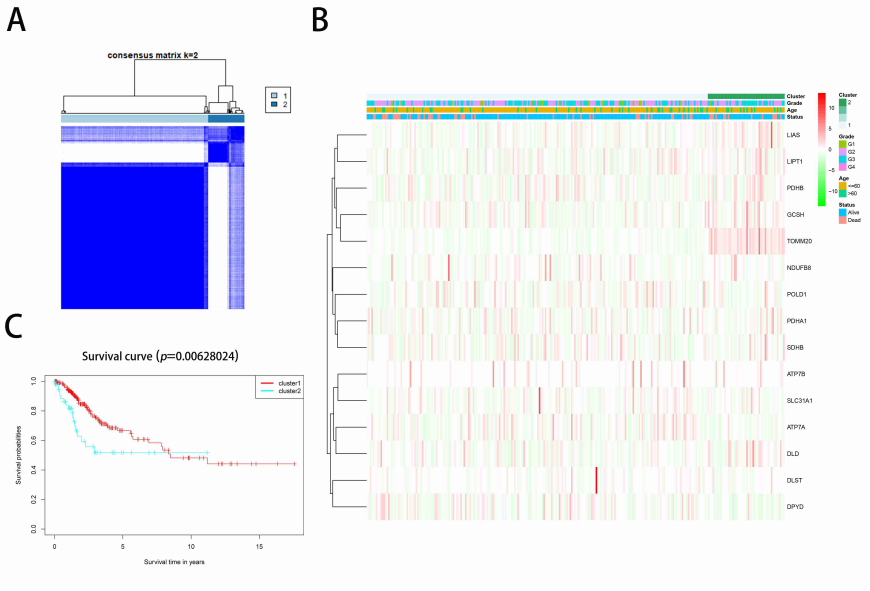

FIGURE 3. Tumor classification based on cuproptosis-associated DEGs. (A) A consensus clustering matrix of 306 CC patients was developed (k = 2). (B) This heatmap shows the clinicopathologic features of two clusters categorized by means of the DEGs (G1, G2 and G3). (C) Kaplan-Meier OS curves.

3.3 Development of a prognostic risk model in TCGA cohort

The survival information of 304 CC samples was matched with corresponding patients. A preliminary screening of survival related genes was conducted by univariate Cox regression analysis. Six genes (*GCSH*, *LIPT1*, *SDHB*, *NDUFB8*, *PDHA1* and *TOMM20*) with $p < 0.2$ were retained, wherein *TOMM20* (95% confidence interval (CI): 1.0045–1.0248, $p = 0.0046$, hazard ratio (HR) = 1.0146) and *PDHA1* (95% CI: 0.9318–0.9930, $p = 0.0168$, HR = 0.9619) had $p < 0.05$ (Fig. 4A). Further assessment revealed two genes (*GCSH* and *TOMM20*) with increased risk while four genes (LIPT1, SDHB, *NDUFB8* and *PDHA1*) have protective relationship (Fig. 4A). The multivariate Cox regression exhibited that *TOMM20* was an independent prognostic factor ($p = 0.0051$, 95% CI: 1.0048–1.0273, HR = 1.0160, Fig. 4B). One 6-gene signature was established *via* LASSO Cox regression analysis (Fig. 4C,D). Risk score was determined as follows: Risk Score = (−0.03537 × *NDUFB8* expression) + (−0.03083 × *PDHA1* expression) + (0.13657 × *GCSH* expression) + (−0.30665 × *LIPT1* expression) + (−0.01115 × *SDHB* expression) + (0.01586 × *TOMM20* expression). Resultantly, 304 patients were divided into two equal low- and high-risk subgroups by their median scores (Fig. 4E). Patients of different risks were divided into two clusters according to principal component analysis (PCA, Fig. 4F). High-risk group compared to low risk had shorter survival time and thus higher death rate (Fig. 4G). Fig. 4H shows that the OS time was different for low-risk and high-risk groups ($p < 0.001$). AUC was calculated from the time-dependent ROC analysis to assess specificity and sensitivity of the prognostic model. AUC reached 0.67 in one year, 0.739 at 2, and 0.688 at 5 (Fig. 4I).

3.4 External validation of risk model in GEO cohort

Sixty-three CC patients from GEO cohort (GSE30759) were included, while the cases with incomplete data were excluded. Forty-eight CC patients were placed in the validation set. Among GEO cohort, twenty-four patients were classified as low risk while twenty-four as high-risk (Fig. 5A). Fig. 5B shows that PCA separated the two subgroups. Patients from low risk subgroups had lower mortality rates and thus longer survival ratios than those from high-risk (Fig. 5C). KM results also reflected an obvious gap in survival for high-risk and low-risk groups ($p = 0.0239$, Fig. 5D). Risk model had great predictive performance as indicated from the ROC curves analysis in GEO cohort (AUC = 0.485 at one year, 0.598 at two and 0.602 at five, Fig. 5E).

3.5 Independent predictive value of the risk model

Univariate and multivariate Cox regression analyses assessed whether the risk score model can function as an independent prognostic factor. Univariate Cox regression analysis of GEO and TCGA cohorts demonstrated that risk score was an independent prognostic factor ($p = 0.0012$, 95% CI: 1.4150–4.0667, HR = 2.3988, and $p = 0.0242$, 95% CI: 1.1379–6.3776, HR = 2.6939, Fig. 6A,B). Multivariate analysis also depicted that the risk score was an independent prognostic factor in GEO and TCGA cohorts ($p < 0.001$, 95% CI: 1.5056–4.3746, HR = 2.5664, and $p = 0.0279$, 95% CI: 1.1172–6.8802, HR = 2.7724, Fig. 6C,D). Moreover, there was difference in the survival status and age of patients at high- and low-risk in the heatmaps (Fig. 6E,F).

3.6 Functional analysis based on the risk model

The "limma" R package was employed to extract DEGs with FDR <0.05 and log2FC >1 for the subgroups classified by prognosis model. In TCGA cohort, 376 DEGs were identified for high- and low-risk groups based on risk score subgroups. Among them, 177 genes were adjusted while 199 were down-regulated. GO enrichment analysis and KEGG pathway analysis were performed based on DEGs. GO analysis revealed that DEGs were linked to the organization of extracellular matrix and its structure in the BP group, collagen-containing extracellular matrix, apical part of cell and apical plasma membrane in the CC component and signaling receptor activator activity in the MF component. From KEGG pathway analysis, the DEGs were associated with cytokine-cytokine receptor interactions and neuroactive ligand-receptor interactions (Fig. 7A,B).

4. Discussion

Several studies had used genes for prognosing CC patients, however few cuproptosis-related genes were systematically used in this regard [17–19]. Their focus was more on the correlation between cuproptosis-related lncRNAs and CC prognosis [20–24]. This work focused on the correlation between cuproptosis-related genes and CC to define the cuproptosis role in CC. The differentially expressed cuproptosis-related genes including six cuproptosis-related risk signatures (*GCSH*, *LIPT1*, *SDHB*, *NDUFB8*, *PDHA1* and *TOMM20*) were utilized to establish one prognostic model. *TOMM20* demonstrated a correlation with survival through multivariate and univariate Cox regression analyses which reflected about its role as autonomous prognostic indicator for CCs. The model herein performed well in multiple Cox regression analyses, univariate and multivariate Cox regressions, K-M survival analysis, and AUC analysis in TCGA and GEO cohorts. This model thus served to evaluate the prognosis-risk categorization and to choose the treatments for CC patients.

The long-term prognosis of patients with recurrent and metastatic CC remained challenging despite the advances in therapeutic strategies including surgery, chemotherapy, radiotherapy, and immunotherapy to treat CC [25]. Cuproptosis is a newly identified form of cellular death and its mechanism is like that of ferroptosis [7]. Tsvetkov *et al.* [7] first proposed cuproptosis as independent death mechanism involving copper and mitochondria. Some studies had explored the effect of copper ionophores such as elesclomol through clinical trials on other cancers [26, 27]. The understanding of cuproptosis was limited regarding the drug mechanism and lack of markers. Exploring the cuproptosis mechanism and cellular copper toxicity might

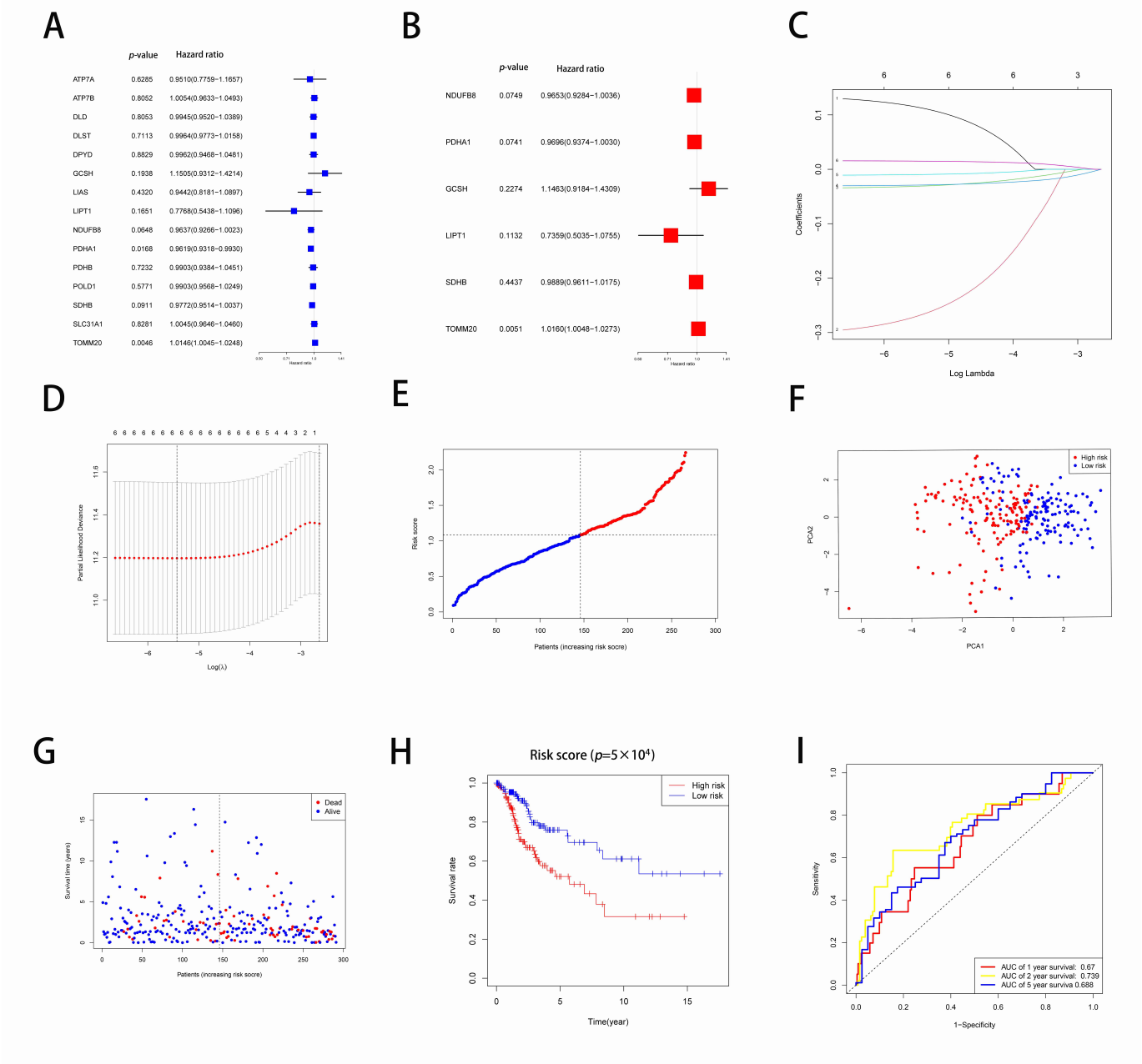

FIGURE 4. The constitution of the TCGA risk signature. (A) Using univariate Cox regression analysis, we examined the OS for every cuproptosis-associated gene together with 6 genes with $p < 0.2$. (B) The six cuproptosis-associated genes were analyzed with multivariate Cox regression. (C) LASSO regression analysis was performed to screen the most helpful prognostic genes. (D) Tuning the parameter (lambda) selection in the regression of LASSO. (E) Allocation of the risk score by the prognostic signature. (F) PCA plot for CCs on the foundation of the risk score. (G) The survival states for all patients. (H) KM curves for the OS of patients in the low- and high-risk communities. (I) ROC curves illuminated the predictive efficiency of the risk score.

help in treating CC patients having resistance to other programmed cell deaths. However, the role and prognostic value of copper mortality in CC was unclear. One prognostic model was thus set up based on six differentially expressed cuproptosis-associated genes of prognostic value. These six genes have been linked to carcinoma. Adamus *et al.* [28] discovered that *GCSH* antisense regulation determined the breast cancer cell viability. Chen *et al.* [29] found that LIPT1 was linked to bladder cancer prognosis and inhibited the migratory ability of bladder cancer cells. Studies had revealed that SDHB was associated with pheochromocytomas. Liu *et al.* [30–34] indicated that miR-142-5p boosted the colorectal carcinoma progression by targeting SDHB and promoting aerobic glycolysis. Chung depicted that *NDUFB8* was linked to the local recurrence-free survival in nasopharyngeal carcinoma. Wang *et al.* [35, 36] reported that γ-tocotrienol impeded the oxidative phosphorylation and caused apoptosis by hampering the mitochondrial compound I subunit *NDUFB8* and compound II subunit SDHB. Zhuang *et al.* [37] stated that exosomal miR-21-5p from SKOV3 ovarian cancer cells being resistant to cisplatin, enhanced the glycolysis and hindered the chemosensitivity of SKOV3 progenitor cells by targeting

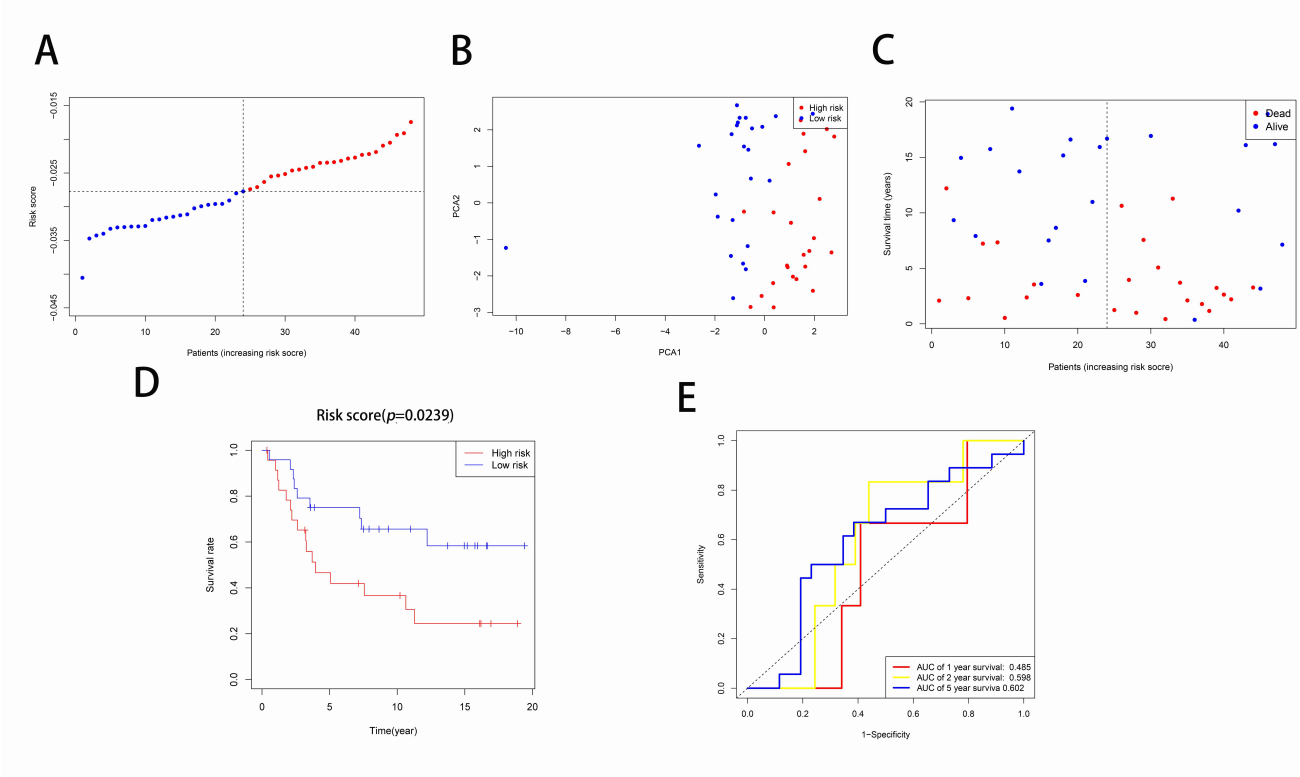

FIGURE 5. Validation of the risk model in the GEO cohort. (A) Patients in the GEO cohort based on their median risk score in the TCGA cohort. (B) PCA plot for CCs. (C) The survival states for all patients. (D) KM curves comparing OS between the high- and low-risk cohorts. (E) The curves of time-dependent ROC for CCs. PCA: principal component analysis; AUC: area under the curve.

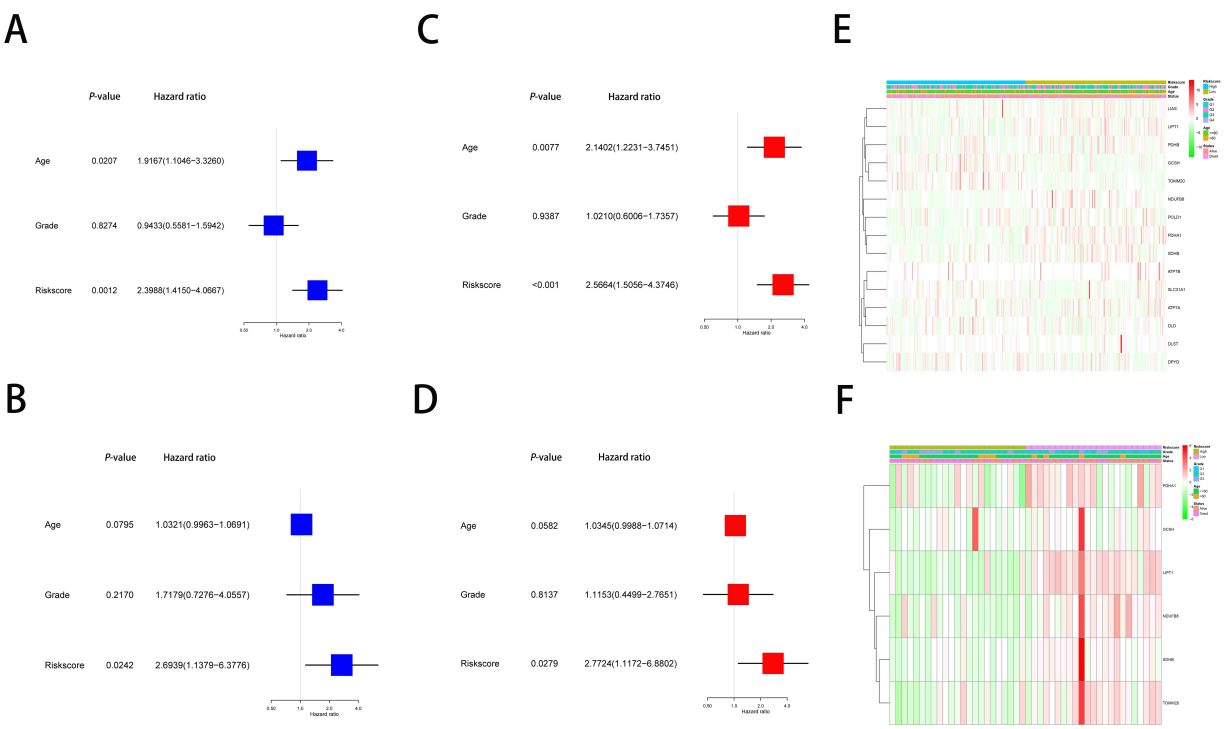

FIGURE 6. Multivariate Cox regression, along with univariate Cox regression according to risk score and clinical characteristics. (A) Univariate analysis of TCGA cohort. (B) Multivariate analysis of the TCGA cohort. (C) Univariate analysis of GEO cohort. (D) Multivariate analysis of GEO cohort. (E) Heatmap of TCGA cohort. (F) Heatmap of the GEO cohort.

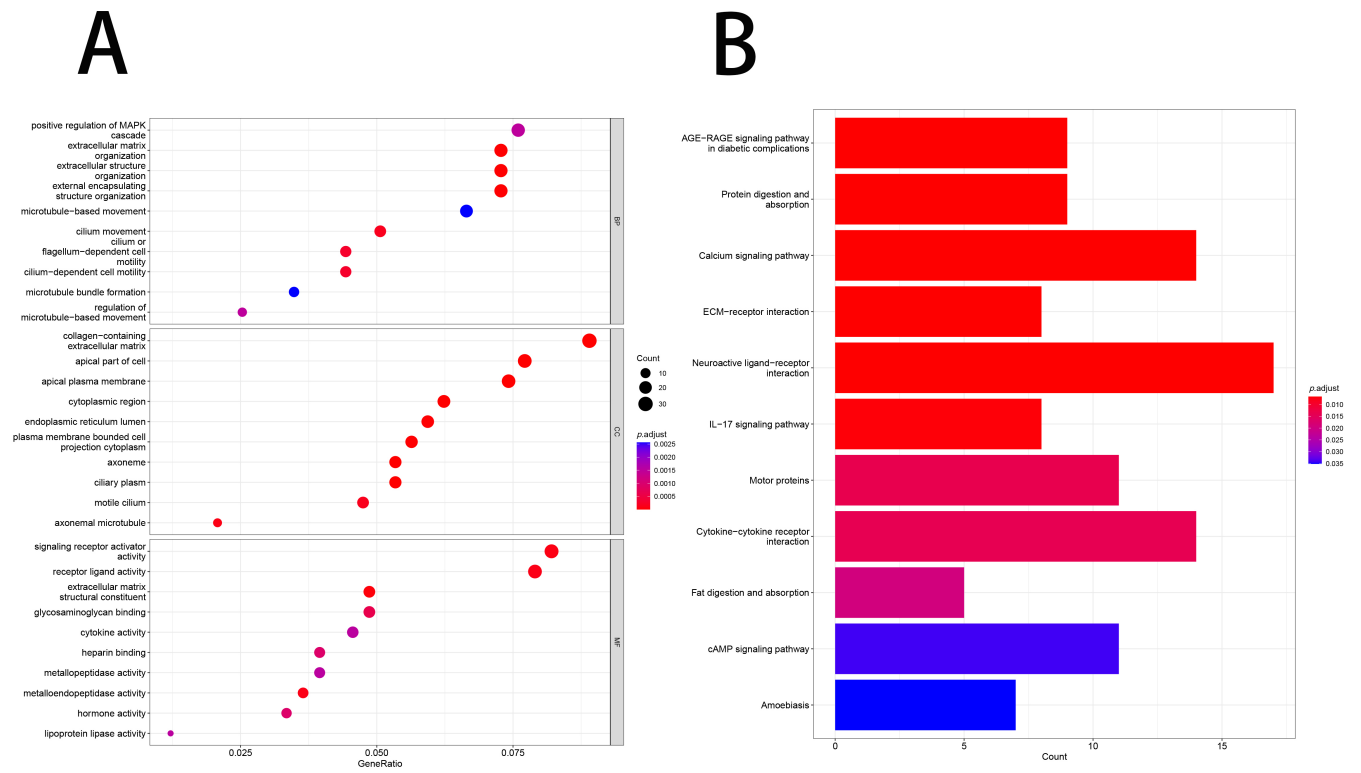

FIGURE 7. Functional analysis of DEGs between cohorts of TCGA. (A) Bubble plot for GO enrichment. (B) Bar plot of the KEGG pathways. AGE: advanced glycation end products; RAGE: receptor for advanced glycation end products; ECM: extra cellular matrix; IL: interleukin.

PDHA1. Liu *et al*. [38] reported that miR-21-5p regulated the glycolysis and cancer progression in gastric carcinoma by targeting *PDHA1*. Roche *et al*. [39] revealed that the translocase of outside mitochondrial membrane compound subunit 20 (*TOMM20*) boosted cancerous aggressiveness and treatment resistance in the chondrosarcoma. Yang *et al*. [40] found that PRR34-AS1 sponges miR-498 promoted *TOMM20*- and *ITGA6*-mediated organism advancement in hepatocellular carcinoma. Moreover, the KEGG and GO function enrichment analyses in this study illustrated that differentially expressed cuproptosis-associated genes were involved in the cellular activity signaling pathways, including extracellular matrix organization and receptor ligand activity in GO, and neuroactive ligand-receptor interaction and cytokine-cytokine receptor interaction in KEGG. These differentially expressed cuproptosis-associated genes participated in several biological functions, and in signaling pathways linked to CCs. Developing a new risk model of cuproptosis was thus important for treating and prognosing cervical cancer.

This research has some limitations. First, the data used in this study originated in public databases, and the sample size was not large. Second, due to some clinical data being lacking, we could not conduct a comprehensive clinical analysis. The third limitation is the technical limitation. Due to the study solely relies on machine learning algorithms without validating performance using clinical samples. Forth, further study like large samples clinical research and basic research are needed to determine the molecular mechanism of cuproptosis affects the prognosis of CCs and the relevance of clinical translational therapy.

5. Conclusions

By utilizing differentially expressed genes associated with cuproptosis, this study effectively developed a risk prediction model that demonstrates exceptional prognostic capabilities for CC. The prognostic model can offer a vital recommendation for future biomarkers, prognosis prediction, and may provide an important direction in therapeutic targets for the precise treatment of cervical cancer.

AVAILABILITY OF DATA AND MATERIALS

The information in this research was obtained from the TCGA database website (https://portal.gdc.cancer.gov/repository), the GTEx database (https://xenabrowser.net/datapages/) and the GEO database (https://www.ncbi.nlm.nih.gov/geo/, ID: GSE30759).

AUTHOR CONTRIBUTIONS

HLS—designed, conducted, and drafted this study. YXC and YSL—revised the paper. MML, XF, HJW, YC and WXL—edited the figures and refined the language. KW and XF—oversaw the total research and made recommendations. It has been watched and approved by the overall writers, who made a contribution to the manuscript vision.

ETHICS APPROVAL AND CONSENT TO PARTICIPATE

Not applicable.

ACKNOWLEDGMENT

Our thanks go out to the TCGA project for its worthy contributions to CC study. It has been a great pleasure to work with the GTEx project on normal cervical samples. We are grateful for its valuable contributions. It is with gratitude that we acknowledge Zhuang J, Jones A, Lee SH, Ng E, and the teams who contributed their data to the GEO database.

FUNDING

This study was sponsored by Tianjin Health Research Project (no. TJWJ2022QN016), Key research project of Hebei Provincial Health (no. 20211024) and the Starting Foundation of MD/Ph.D. and Introduced Talent issued by Tianjin Medical University Cancer Institute and Hospital (no. B2113).

CONFLICT OF INTEREST

The authors declare no conflict of interest.

REFERENCES

[1] Arbyn M, Weiderpass E, Bruni L, de Sanjosé S, Saraiya M, Ferlay J, *et al*. Estimates of incidence and mortality of cervical cancer in 2018: a worldwide analysis. The Lancet Global Health. 2020; 8: e191–e203.

[2] Siegel RL, Miller KD, Fuchs HE, Jemal A. Cancer statistics, 2021. CA: A Cancer Journal for Clinicians. 2021; 71: 7–33.

[3] Jin J. HPV infection and cancer. JAMA. 2018; 319: 1058.

[4] Sung H, Ferlay J, Siegel RL, Laversanne M, Soerjomataram I, Jemal A, *et al*. Global cancer statistics 2020: GLOBOCAN estimates of incidence and mortality worldwide for 36 cancers in 185 countries. CA: A Cancer Journal for Clinicians. 2021; 71: 209–249.

[5] Bjurberg M, Beskow C, Kannisto P, Lindahl G. Cervical cancer is a clinical challenge. Läkartidningen. 2015; 112: DIUS. (In Swedish)

[6] Pimple SA, Mishra GA. Global strategies for cervical cancer prevention and screening. Minerva Ginecologica. 2019; 71: 313–320.

[7] Tsvetkov P, Coy S, Petrova B, Dreishpoon M, Verma A, Abdusamad M, *et al*. Copper induces cell death by targeting lipoylated TCA cycle proteins. Science. 2022; 375: 1254–1261.

[8] Ou R, Lu S, Wang L, Wang Y, Lv M, Li T, *et al*. Circular RNA circLMO1 suppresses cervical cancer growth and metastasis by triggering miR-4291/ACSL4-mediated ferroptosis. Frontiers in Oncology. 2022; 12: 858598.

[9] Ye Y, Dai Q, Qi H. A novel defined pyroptosis-related gene signature for predicting the prognosis of ovarian cancer. Cell Death Discovery. 2021; 7: 71.

[10] Song H, Li T, Sheng J, Li D, Liu X, Xiao H, *et al*. Necroptosis-related miRNA biomarkers for predicting overall survival outcomes for endometrial cancer. Frontiers in Genetics. 2022; 13: 828456.

[11] Dixon SJ, Lemberg KM, Lamprecht MR, Skouta R, Zaitsev EM, Gleason CE, *et al*. Ferroptosis: an iron-dependent form of nonapoptotic cell death. Cell. 2012; 149: 1060–1072.

[12] Tsvetkov P, Detappe A, Cai K, Keys HR, Brune Z, Ying W, *et al*. Mitochondrial metabolism promotes adaptation to proteotoxic stress. Nature Chemical Biology. 2019; 15: 681–689.

[13] Wang Y, Zhang L, Zhou F. Cuproptosis: a new form of programmed cell death. Cellular & Molecular Immunology. 2022; 19: 867–868.

[14] Tang D, Chen X, Kroemer G. Cuproptosis: a copper-triggered modality of mitochondrial cell death. Cell Research. 2022; 32: 417–418.

[15] Jiang Y, Huo Z, Qi X, Zuo T, Wu Z. Copper-induced tumor cell death mechanisms and antitumor theragnostic applications of copper complexes. Nanomedicine. 2022; 17: 303–324.

[16] Yu G, Wang LG, Han Y, He QY. clusterProfiler: an R package for comparing biological themes among gene clusters. OMICS: a Journal of Integrative Biology. 2012; 16: 284–287.

[17] Liang B, Li Y, Wang T. A three miRNAs signature predicts survival in cervical cancer using bioinformatics analysis. Scientific Reports. 2017; 7: 5624.

[18] Dai F, Chen G, Wang Y, Zhang L, Long Y, Yuan M, *et al*. Identification of candidate biomarkers correlated with the diagnosis and prognosis of cervical cancer *via* integrated bioinformatics analysis. OncoTargets and Therapy. 2019; 12: 4517–4532.

[19] Ma X, Liu J, Wang H, Jiang Y, Wan Y, Xia Y, *et al*. Identification of crucial aberrantly methylated and differentially expressed genes related to cervical cancer using an integrated bioinformatics analysis. Bioscience Reports. 2020; 40: BSR20194365.

[20] Liu X, Zhou L, Gao M, Dong S, Hu Y, Hu C. Signature of seven cuproptosis-related lncRNAs as a novel biomarker to predict prognosis and therapeutic response in cervical cancer. Frontiers in Genetics. 2022; 13: 989646.

[21] Kong X, Xiong Y, Xue M, He J, Lu Q, Chen M, *et al*. Identification of cuproptosis-related lncRNA for predicting prognosis and immunotherapeutic response in cervical cancer. Scientific Reports. 2023; 13: 10697.

[22] Wang Q, Xu Y. Comprehensive analysis of cuproptosis-related lncRNAs model in tumor immune microenvironment and prognostic value of cervical cancer. Frontiers in Pharmacology. 2022; 13: 1065701.

[23] Liu L, Zheng J, Xia H, Wu Q, Cai X, Ji L, *et al*. Construction and comprehensive analysis of a cuproptosis-related lncRNA signature for predicting prognosis and immune response in cervical cancer. Frontiers in Genetics. 2023; 14: 1023613.

[24] Zhou J, Xu L, Zhou H, Wang J, Xing X. Prediction of prognosis and chemotherapeutic sensitivity based on cuproptosis-associated lncRNAs in cervical squamous cell carcinoma and endocervical adenocarcinoma. Genes. 2023; 14: 1381.

[25] Liu Y, Fan Y, Wang X, Huang Z, Shi K, Zhou B. Musashi-2 is a prognostic marker for the survival of patients with cervical cancer. Oncology Letters. 2018; 15: 5425–5432.

[26] Monk BJ, Kauderer JT, Moxley KM, Bonebrake AJ, Dewdney SB, Secord AA, *et al*. A phase II evaluation of elesclomol sodium and weekly paclitaxel in the treatment of recurrent or persistent platinum-resistant ovarian, fallopian tube or primary peritoneal cancer: an NRG oncology/gynecologic oncology group study. Gynecologic Oncology. 2018; 151: 422–427.

[27] O'Day SJ, Eggermont AM, Chiarion-Sileni V, Kefford R, Grob JJ, Mortier L, *et al*. Final results of phase III SYMMETRY study: randomized, double-blind trial of Elesclomol plus paclitaxel versus paclitaxel alone as treatment for chemotherapy-naive patients with advanced melanoma. Journal of Clinical Oncology. 2013; 31: 1211–1218.

[28] Adamus A, Müller P, Nissen B, Kasten A, Timm S, Bauwe H, *et al*. GCSH antisense regulation determines breast cancer cells' viability. Scientific Reports. 2018; 8: 15399.

[29] Chen Y, Xu T, Xie F, Wang L, Liang Z, Li D, *et al*. Evaluating the biological functions of the prognostic genes identified by the pathology atlas in bladder cancer. Oncology Reports. 2021; 45: 191–201.

[30] Li H, Hardin H, Zaeem M, Huang W, Hu R, Lloyd RV. LncRNA expression and SDHB mutations in pheochromocytomas and paragangliomas. Annals of Diagnostic Pathology. 2021; 55: 151801.

[31] Buffet A, Burnichon N, Favier J, Gimenez-Roqueplo A. An overview of 20 years of genetic studies in pheochromocytoma and paraganglioma. Best Practice & Research Clinical Endocrinology & Metabolism. 2020; 34: 101416.

[32] Jochmanova I, Wolf KI, King KS, Nambuba J, Wesley R, Martucci V, *et al*. SDHB-related pheochromocytoma and paraganglioma penetrance and genotype-phenotype correlations. Journal of Cancer Research and Clinical Oncology. 2017; 143: 1421–1435.

[33] Jochmanova I, Abcede AMT, Guerrero RJS, Malong CLP, Wesley R, Huynh T, *et al*. Clinical characteristics and outcomes of SDHB-related pheochromocytoma and paraganglioma in children and adolescents.

Journal of Cancer Research and Clinical Oncology. 2020; 146: 1051–1063.

[34] Liu S, Xiao Z, Ai F, Liu F, Chen X, Cao K, *et al*. miR-142-5p promotes development of colorectal cancer through targeting SDHB and facilitating generation of aerobic glycolysis. Biomedicine & Pharmacotherapy. 2017; 92: 1119–1127.

[35] Chung IC, Chen LC, Tsang NM, Chuang WY, Liao TC, Yuan SN, *et al*. Mitochondrial oxidative phosphorylation complex regulates NLRP3 inflammasome activation and predicts patient survival in nasopharyngeal carcinoma. Molecular & Cellular Proteomics. 2020; 19: 142–154.

[36] Wang H, Luo J, Tian W, Yan W, Ge S, Zhang Y, *et al*. γ-Tocotrienol inhibits oxidative phosphorylation and triggers apoptosis by inhibiting mitochondrial complex I subunit NDUFB8 and complex II subunit SDHB. Toxicology. 2019; 417: 42–53.

[37] Zhuang L, Zhang B, Liu X, Lin L, Wang L, Hong Z, *et al*. Exosomal miR-21-5p derived from cisplatin-resistant SKOV3 ovarian cancer cells promotes glycolysis and inhibits chemosensitivity of its progenitor SKOV3 cells by targeting PDHA1. Cell Biology International. 2021; 45: 2140–2149.

[38] Liu Z, Yu M, Fei B, Fang X, Ma T, Wang D. miR-21-5p targets PDHA1 to regulate glycolysis and cancer progression in gastric cancer. Oncology Reports. 2018; 40: 2955–2963.

[39] Roche ME, Lin Z, Whitaker-Menezes D, Zhan T, Szuhai K, Bovee JVMG, *et al*. Translocase of the outer mitochondrial membrane complex subunit 20 (TOMM20) facilitates cancer aggressiveness and therapeutic resistance in chondrosarcoma. Biochimica Et Biophysica Acta (BBA)—Molecular Basis of Disease. 2020; 1866: 165962.

[40] Yang X, Song D, Zhang J, Yang X, Feng H, Guo J. PRR34-AS1 sponges miR-498 to facilitate TOMM20 and ITGA6 mediated tumor progression in HCC. Experimental and Molecular Pathology. 2021; 120: 104620.

How to cite this article: Hualin Song, Yanxiang Cao, Yishuai Li, Miaomiao Liu, Huijuan Wu, Ying Chen, *et al*. Cuproptosis-related gene biomarkers to predict overall survival outcomes in cervical cancer. European Journal of Gynaecological Oncology. 2025; 46(4): 25-34. doi: 10.22514/ejgo.2025.048.